



Published in final edited form as:

*Neurobiol Aging*. 2012 February ; 33(2): 422.e11–422.e25. doi:10.1016/j.neurobiolaging.2010.09.017.

## CCAAT/enhancer binding protein delta (CEBPD) elevating PTX3 expression inhibits macrophage-mediated phagocytosis of dying neuron cells

Chiung-Yuan Ko<sup>a,1</sup>, Ling-Hua Chang<sup>b,1</sup>, Yi-Chao Lee<sup>c,1</sup>, Esta Sterneck<sup>d,1</sup>, Chun-Pei Cheng<sup>e</sup>, Shun-Hua Chen<sup>f</sup>, A-Mei Huang<sup>g</sup>, Joseph T. Tseng<sup>e</sup>, and Ju-Ming Wang<sup>a,e,h,\*</sup>

<sup>a</sup>Center for Gene Regulation and Signal Transduction Research, National Cheng Kung University, Tainan, Taiwan

<sup>b</sup>Institute of Basic Medical Sciences, College of Medicine, National Cheng Kung University, Tainan, Taiwan

<sup>c</sup>Department of Pharmacology, National Cheng Kung University, Tainan, Taiwan

<sup>d</sup>Center for Cancer Research, National Cancer Institute, Frederick, MD, USA

<sup>e</sup>Institute of Bioinformatics, College of Bioscience and Biotechnology, National Cheng Kung University, Tainan, Taiwan

<sup>f</sup>Department of Microbiology and Immunology, National Cheng Kung University, Tainan, Taiwan

<sup>g</sup>Department of Biochemistry, Kaohsiung Medical University, Kaohsiung, Taiwan

<sup>h</sup>Institute of Biosignal Transduction, College of Bioscience and Biotechnology, National Cheng Kung University, Tainan, Taiwan

### Abstract

The CCAAT/enhancer binding protein delta (CEBPD, C/EBP $\delta$ , NF-IL6 $\beta$ ) is induced in many inflammation-related diseases, suggesting that CEBPD and its downstream targets may play central roles in these conditions. Neuropathological studies show that a neuroinflammatory response parallels the early stages of Alzheimer's disease (AD). However, the precise mechanistic correlation between inflammation and AD pathogenesis remains unclear. CEBPD is upregulated in the astrocytes of AD patients. Therefore, we asked if activation of astrocytic CEBPD could contribute to AD pathogenesis. In this report, a novel role of CEBPD in attenuating macrophage-mediated phagocytosis of damaged neuron cells was found. By global gene expression profiling, we identified the inflammatory marker pentraxin-3 (PTX3, TNFAIP5, TSG-14) as a CEBPD target in astrocytes. Furthermore, we demonstrate that PTX3 participates in the attenuation of macrophage-mediated phagocytosis of damaged neuron cells. This study provides the first

\*Corresponding author at: Institute of Biosignal Transduction, College of Bioscience and Biotechnology, National Cheng Kung University, Tainan 70101, Taiwan. Tel.: +886 6 2757575 × 31067; fax: +886 6 208366. yumingw@mail.ncku.edu.tw (J.-M. Wang).

<sup>†</sup>These authors contributed equally to this study.

#### Disclosure statement

None of the authors has a conflict of interest to declare in relation to the present research.

#### Appendix A. Supplementary data

Supplementary data associated with this article can be found, in the online version, at doi:10.1016/j.neurobiolaging.2010.09.017.

demonstration of a role for astrocytic CEBPD and the CEBPD-regulated molecule PTX3 in the accumulation of damaged neurons, which is a hallmark of AD pathogenesis.

## Keywords

CEBPD; PTX3; Alzheimer's disease; Phagocytosis

---

## 1. Introduction

Alzheimer's disease (AD) is a neurodegenerative disease that occurs predominantly in elderly people and leads to behavioral changes, including impaired memory and learning as well as cognitive loss. It has been shown that senile plaques are a pathologic hallmark of AD and are composed of  $\beta$ -amyloid ( $A\beta$ ), activated microglia, astrocytes, and degenerating neurons (Giulian et al., 1995; Itagaki et al., 1989; Sasaki et al., 1997; Streit et al., 2004). Two pathologic lesions are present: amyloid plaques and neurofibrillary tangles (NFTs). These insoluble aggregates of protein accumulate both inside and outside neurons. Other neuropathological features that accompany the progression of AD include a decrease in synaptic density, dystrophic neurites, inflammation, and neuronal cell loss. Inflammation can be autotoxic to neurons, exacerbating the fundamental failure underlying the neurological disorder. Microglia, which are highly reactive to environmental changes, are the principal immune cells of the brain. However, the exact role of microglia in the pathogenesis of AD has not yet been resolved. Interestingly, the phenomenon of the atypical inflammatory response has parallels with the phagocytosis of apoptotic neuron cells in macrophages, which is seen in some brain and neurodegenerative diseases (Cole et al., 2006; Staikos et al., 2008). The astrocytes also generate a response of the brain to injury through production of growth factors, which can further promote microglial growth and activation or modulate the cytotoxic activity (Lee et al., 1994; Martin et al., 1994). Therefore, microglial cells and astrocytes are important for understanding the pathogenesis of AD.

The lesions observed in AD are characterized by the existence of inflammatory mediators, such as cytokines, chemokines, proteases, free radicals, pentraxins, and activated complement proteins (McGeer and McGeer, 1995, 2002). Several factors involved in inflammatory reactions have been implicated in both astrocyte and microglia functions (Bonifati and Kishore, 2007; Qin et al., 2008). However, the regulation of these immune factors and their functional significance in disease-relevant processes such as macrophage-mediated phagocytosis of dead neurons remain unclear.

The inflammatory marker pentraxin-3 (PTX3) is a secreted molecule, which consists of a C-terminal domain similar to classical pentraxins (e.g., C-reactive protein [CRP]) and of an unrelated N-terminal domain. PTX3 is produced and released in situ by many different cell types including dendritic cells, macrophages, fibroblasts, activated endothelial cells, and neutrophils (Ortega-Hernandez et al., 2009). The production of PTX3 can be stimulated by lipopolysaccharide (LPS), interleukin-1 beta (IL-1 $\beta$ ), interleukin-10 (IL-10), and tumor necrosis factor- $\alpha$  (TNF- $\alpha$ ) (Altmeyer et al., 1995; Basile et al., 1997; Breviario et al., 1992; Castelo-Branco et al., 2003). PTX3 has functional roles in the innate resistance against

selected pathogens, and also in regulating inflammatory reactions and autoimmunity, by assuming antibody-like functions such as facilitating pathogen recognition by phagocytes (Bottazzi et al., 2006; Mantovani et al., 2003). By contrast, complement component 1, q subcomponent (C1q)-enhanced PTX3 can directly bind to the membrane of apoptotic cells, and inhibit the phagocytosis of apoptotic cells by dendritic cells and macrophages (van Rossum et al., 2004). To date, nothing is known about the regulation and function of PTX3 in brain inflammation.

In this study, we show that PTX3 is activated in astrocytes by the transcription factor CCAAT/enhancer binding protein delta (CEBPD; also known as C/EBPdelta, CRP3, CELF, and NF-IL6 $\beta$ ). CEBPD is known to regulate or coregulate a wide range of inflammatory mediators and participate in signaling by IL-1 $\beta$ , interleukin-6 (IL-6), and TNF- $\alpha$  (Cardinaux et al., 2000; Ramji et al., 1993; Tsukada et al., 1994). Induction of CEBPD expression was observed in age-associated disorders such as neuron degeneration (Li et al., 2004), atherosclerosis (Takata et al., 2002), type 2 diabetes (Gao et al., 2006), and rheumatoid arthritis (Nishioka et al., 2000). However, the physiological function of CEBPD and its downstream targets in these inflammation-related diseases are poorly understood. Furthermore, IL-1 $\beta$ , IL-6, and TNF- $\alpha$  are well known to be increased in pathological regions of neurodegeneration, including AD and Parkinson's disease (Glass et al., 2010). Recently, the immunohistochemistry of AD demonstrates the accumulation of CEBPD in reactive astrocytes surrounding A $\beta$  peptide deposits (Li et al., 2004). Therefore, we hypothesized that understanding the roles and downstream targets of astrocytic CEBPD may be important for elucidating the biology of AD pathogenesis. Our results implicate CEBPD-activated PTX3 in the failure of macrophages to remove damaged neurons, which may be 1 mechanism by which inflammation contributes to the development of AD.

## 2. Methods

### 2.1. Materials

Antibodies against hemagglutinin (HA) and  $\beta$ -actin were purchased from BABCO (Richmond, CA, USA) and Sigma (St. Louis, MO, USA), respectively. An antibody against CEBPD (sc-636) for chromatin immunoprecipitation (ChIP) was purchased from Santa Cruz Biotechnology (Santa Cruz, CA, USA). The TRIzol ribonucleic acid extraction reagent, Lipofectamine 2000, Dulbecco's modified Eagle's medium (DMEM), SuperScript<sup>TM</sup> III, and Opti-MEM medium were obtained from Invitrogen (Carlsbad, CA, USA). All oligonucleotides were synthesized by MDBio, Inc. (Taipei, Taiwan). Fetal bovine serum (FBS) was purchased from Hy-Clone Laboratories (Logan, UT, USA). The zinc-inducible CEBPD expression vector, pMT/HA-CEBPD, was constructed by cloning CEBPD complementary DNA (cDNA) with *Bam*HI and *Hind*III into the pMTCB6+ vector (a gift from Dr. Sigal Gery, Cedars-Sinai Medical Center, Los Angeles, CA, USA). For the dominant negative CEBPD expression vector (CEBPD<sup>DN</sup>), the *Not*I/Klenow/*Sal*I fragment of CEBPD cDNA was inserted into the pCDNA3/HA vector by *Bam*HI/Klenow/*Sal*I, which results in an N-terminal deletion of amino acids 2–150 from the CEBPD expression vector.

## 2.2. Cell culture

U373MG (human glioblastoma-astrocytoma cell line), SHSY5Y (human neuroblastoma cell line), and THP-1 (human acute monocytic leukemia cell line) were cultured in DMEM, DMEM/F-12, and RPMI-1640, respectively, containing 5% fetal bovine serum, 100  $\mu\text{g}$  mL streptomycin, and 100 units mL penicillin. For inducible expression of CEBPD, the pMT/HA-CEBPD construct was introduced into U373MG cells and stable clones were selected by G418-resistance. For differentiation of macrophages, THP-1 cells were seeded in 24-well plates and treated with 5 ng/mL phorbol 12-myristate 13-acetate (PMA) for 48 hours first, followed by 7 days of culture without PMA, and medium exchange on day 2 and 5. Mouse embryo fibroblast (MEF) were isolated essentially as described (Tessarollo, 2001) from individual E13.5–E14.5 embryos generated by mating of *Cebpd* null heterozygous mice (Sterneck et al., 1998) of the 129S1 strain. The MEF cells were further immortalized by E1A. These cells were maintained in DMEM/10% FBS and passaged every 3 days at  $3 \times 10^5$  cells per 10 cm dish (3T3 protocol). The 2 established cell lines per genotype were derived from pooled knockout (KO) and wild type (WT) embryos of 2 independent litters each.

## 2.3. AD transgenic mouse

Cortex from 10-month-old APP<sub>Swe</sub> + PS1/E9 bigenic mice obtained from Jackson Laboratory (Bar Harbor, ME, USA; stock no. 004462) was homogenized in 1 mL phosphate buffered saline (PBS), including 10 mM sodium fluoride (NaF), 1 mM phenylmethylsulfonyl fluoride (PMSF), aprotinin, 1  $\mu\text{g}$  mL leupeptin 1  $\mu\text{g}$ /mL, and 1 mM sodium orthovanadate (Na<sub>3</sub>VO<sub>4</sub>). After centrifugation, the supernatant was stored at  $-80^\circ\text{C}$  for further analysis.

## 2.4. Culture of primary cortical neurons, mixed glial cells, and A $\beta$ treatment

Mouse cortical neurons were established from cerebral hemispheres of postnatal day 0 (P0) C57BL/6 mouse pups. The cortex was dissected and digested in 7 mL of trypsin (10 units/mL) in PBS at  $37^\circ\text{C}$  for 30 minutes. After rinsing, the tissue was triturated and filtered through a nylon mesh filter (70  $\mu\text{m}$ ). Cells were plated at  $0.5 \times 10^6$  cells/cm<sup>2</sup> onto a plastic culture plate coated with poly-L-lysine and maintained in Neurobasal A medium supplemented with 100 U/mL penicillin, 0.1 mg/mL streptomycin, 0.5 mM L-glutamine, and 5% FBS (Invitrogen). The next day, 8  $\mu\text{M}$  cytosine arabinoside (Ara-C; Invitrogen) was added to prevent glial cell growth. By glial fibrillary acidic protein (GFAP) immunostaining (Invitrogen), the proportion of glial cell was <5% of the total population of primary cortical cultured cells. For mixed glial cell cultures the cortex was isolated and prepared as above. However, cells were plated at  $2 \times 10^5$  cells/cm<sup>2</sup> onto a plastic culture plate coated with poly-L-lysine and maintained in DMEM/F12 medium supplemented with 10% FBS and 100 units mL penicillin. The A $\beta$  aggregate was prepared from a solution of 1 mM of soluble A $\beta$ <sub>(1–42)</sub> (Sigma, St. Louis, MO, USA) in 0.01 M PBS (pH 7.4). The solution was incubated at  $37^\circ\text{C}$  for 3 days to form the aggregated A $\beta$  and stored at  $-70^\circ\text{C}$ . Cells were treated with 5  $\mu\text{M}$  A $\beta$ <sub>(1–42)</sub> for 24 hours.

## 2.5. Human PTX3 promoter cloning and mutagenesis

The 5'-flanking region of *PTX3* gene was obtained from THP-1 cells by using the DNeasy Tissue Kit (Qiagen, Düsseldorf, Germany) and a forward primer, 5'-GGTACCTAATA-ACCCCTATCTCACTT-3', and reverse primer, 5'-AAGCTTCTGAGTTTGAGCGGAGGAGA-3. The 5'-serial deletion mutants of *PTX3* promoter were generated by polymerase chain reaction (PCR) with above reverse primer and the following forward primers: PTX3/-473KpnI: 5'-GGTACCTTGGACTTGACTTTCAGAGC-3', or PTX3/-44KpnI: 5'-GGTACCTGCCACCAGCATTACTCATT-3'. These verified fragments were digested with *KpnI* and *HindIII* and then subcloned into promoter-less PGL2-basic vector. Mutant reporter plasmids were derived from -473/+60 wt reporter by site-directed mutagenesis following the instructions of the QuikChange Site-directed Mutagenesis Kit (Stratagene, CA, USA) with the M1 (5'-TTTGCGGTTTAATATCTCGAGACTTCCACATTTCCC-3') or M5 (5'-CTATATA-TAAAGGGTCTCGAGATAATAACAGCTCAC-3') primers.

## 2.6. Plasmid transfection and reporter gene assay

To analyze the promoter activity of *PTX3* reporters, U373MG cells were transiently transfected with plasmids as indicated by Lipofectamine 2000 according to the manufacturer's instructions. The total DNA amount for each experiment was kept constant with control empty vectors. After 6 hours of incubation with transfection mixtures, the Opti-MEM medium was changed to regular medium and incubated for a further 12 hours. Luciferase activities of transfectants were measured by the Luciferase Assay System (Promega, Madison, WI, USA) according to the manufacturer's instructions.

## 2.7. Microarray analysis and reverse transcription-PCR (RT-PCR)

Total RNAs were isolated using the TRIzol RNA extraction reagent. Samples were validated with Agilent Human Whole Genome Oligo 4 × 44 K Microarray (Welgene Biotech. Co., Taipei, Taiwan), following the manufacturers' protocols. All processes were performed by Welgene Biotech Company (Taipei, Taiwan). Good quality signals were obtained by filtering for scores of *p*-value < 0.05 in all replicates, M-value of > 6 in all signals, and more than 1.5-fold change. Finally, the function of candidate genes was assigned by Ingenuity Pathway Analysis (IPA) (Ingenuity Systems Inc., Redwood City, CA, USA). For RTPCR, total RNA was isolated as mentioned above, and subjected to reverse transcription with SuperScript™ III. Specific primers for RT-PCR in this study are shown in Supplemental Table 1. The PCR products were separated by electrophoresis in 2% agarose gels and visualized with ethidium bromide staining.

## 2.8. Program of prediction of CEBPD binding motifs (PCDBM)

The promoter sequences of human, rat, and mouse genes were retrieved by the EnsMart System ([www.ensembl.org/biomart/martview/c6c926d9815de045873590a6da1ac151](http://www.ensembl.org/biomart/martview/c6c926d9815de045873590a6da1ac151)). To allow user-directed analysis of promoter sequences and obtain prediction of putative CEBPD-specific binding motif, the free web site of PCDBM was constructed following the report of S. Osada et al. (Osada et al., 1996). The 5'-flanking region of genes can be extracted and down-loaded in a FASTA format cluster. With the php ([www.php.net](http://www.php.net)) and

MySQL ([www.mysql.com](http://www.mysql.com)) free database systems for constructing a web service bioinformatic tool, all the data were imported into the MySQL database. In addition, the binding predictions for CEBPB and CEBPA also are available in the output frame for reference.

## 2.9. Western blot analysis

For Western analysis, cells were lysed with modified radioimmunoprecipitation assay buffer, including 50 mM Tris-HCl (pH 7.4), 150 mM sodium chloride (NaCl), 1 mM ethylenediamine tetraacetic acid (EDTA), 1% NP40, 0.25% sodium deoxycholate (NaDOC), 1 mM dithiothreitol (DTT), 10 mM NaF, 1 mM PMSF, aprotinin, 1  $\mu$ g/mL, leupeptin 1  $\mu$ g/mL, and 1 mM  $\text{Na}_3\text{VO}_4$ . Lysates were resolved on a sodium dodecyl sulfate (SDS)-containing 10% polyacrylamide gel, transferred to polyvinylidene difluoride (PVDF) nylon membrane, and probed with specific antibodies at 4 °C overnight. Specific bands were detected by a horseradish peroxidase-conjugated antibody and revealed by an enhanced chemiluminescence (ECL) Western blot system from Pierce (Rockford, IL, USA).

## 2.10. Short hairpin RNA (shRNA) assay

The lentiviral expression vectors pLKO.1-shLuc and pLKO.1-shCEBPD were purchased from the National RNAi Core Facility located at the Genomic Research Center of Institute of Molecular Biology, Academia Sinica. The effects of a short hairpin RNA (shRNA) designed against luciferase (pLKO.1-shLuc, CTTCGAAATGTCCGTTCCGGTT) as control and against CEBPD (pLKO.1-shCEBPD, GCCGACCTCTTCAACAGCAAT) cloned into pLKO.1 on CEBPD expression levels were determined. Virus was produced as described using Lipofectamine 2000 to cotransfect Phoenix cells with the pLKO.1-shLuc or pLKO.1-shCEBPD vectors together with pMD2.G and psPAX2. Viral supernatants were harvested in the conditioned medium.

## 2.11. Gel shift assay

The  $^{32}\text{P}$ -labeled oligonucleotide probes (0.2 to 0.5 ng) containing the individual putative CEBPD motifs were incubated with 1  $\mu\text{L}$  of in vitro-translated HA-CEBPD in specific binding buffer, as described below, containing 1  $\mu\text{g}$  of poly(dI-dC). After 20 minutes of incubation at room temperature, the reaction mixtures were resolved in a 5% native polyacrylamide gel (with an acrylamide/bisacrylamide ratio of 30:1) at 4 °C, and the specific protein complexes were visualized by autoradiography. The binding buffer contained 10 mM Tris-HCl (pH 7.5), 50 mM NaCl, 1 mM DTT, 1 mM EDTA, and 10% vol/vol glycerol. For the antibody supershift experiments, 1  $\mu\text{g}$  of antibodies against CEBPD was included in the binding reaction mixture. The sense strand sequences of various oligonucleotides used were site 1: 5'-TTTAATATTGTGCAACTTCCAC-3'; site 2: 5'-ATTCAAATTACAACAGCTAATT-3'; site 3: 5'-TGATGATTGCTTCAGTACCCT-3'; site 4: 5'-CAGAAAATGCTGAAATGATGAT-3'; site 5: 5'-TAAAGGGTTGTGAAATAATAAC-3'; and site 6: 5'-TACCAAGTTATGAAAAGAAACA-3'.

### 2.12. Chromatin immunoprecipitation (ChIP) assay

The chromatin immunoprecipitation (ChIP) assay was carried out essentially as described by Wang et al. (2006). Briefly, U373MG and THP-1 cells were treated with 1% formaldehyde for 15 minutes. The cross-linked chromatin was then prepared and sonicated to an average size of 500 bp. The DNA fragments were immunoprecipitated with antibodies specific for CEBPD, or control rabbit immunoglobulin G (IgG) at 4 °C overnight. After reversal of the cross-linking, the immunoprecipitated chromatin was amplified by primers related to the specific regions of the *PTX3* genomic locus. The primers were F-473(S) (5'-GGTACCTTGGACTTGACTTTCAGAGC-3') and R+60(AS) (5'-AAGCTTCTGAGTTTGAGCGGAGGAGA-3'). The amplified DNA products were resolved by agarose gel electrophoresis and confirmed by sequencing.

### 2.13. Phagocytosis assay

Apoptosis was triggered by C-band ultraviolet light (UVC) irradiation (254-nm wavelength) of cells at the dose of 8 mJ/cm<sup>2</sup> followed by incubation of irradiated cells for up to 24 hours. Induction and phase of apoptosis were verified by flow cytometry (quantification confirmed up to 80% cell death) using fluorescein isothiocyanate (FITC)-conjugated annexin V and propidium iodide (PI). The apoptotic SH-SY5Y cells or primary neurons were labeled with PKH-26 red fluorescent cell linker kit (Sigma, St. Louis, MO, USA) according to the manufacturer's instructions. Labeled apoptotic, viable SHSY5Y cells or primary neurons ( $5 \times 10^5$ ) were incubated with various concentrations of recombinant human PTX3 protein or conditioned medium as indicated for 30 minutes at room temperature in a final volume of 50  $\mu$ L PBS containing bovine serum albumin (0.1%). Cells were then washed with PBS and were resuspended in RPMI medium containing 30% FBS. Next, the suspensions (0.3 mL/well) containing  $5 \times 10^5$  SHSY5Y cells or primary neurons were added to the 24-well plates containing monocyte-derived macrophages ( $5 \times 10^4$ /well), and cell interaction was allowed for 30 minutes at 37 °C in 5% CO<sub>2</sub>. Cells were adhered to poly-L-lysine coated coverslips for immunofluorescence analysis or trypsinized for quantitative analysis by flow cytometry. Cells were then stained with anti-F4/80 rat monoclonal antibody (Santa Cruz, Santa Cruz, CA, USA) as a marker for macrophage and secondary goat anti-rat IgG-FITC (Santa Cruz, Santa Cruz, CA, USA). Nuclei were counterstained with 4,6-diamidino-2-phenylindole, dihydrochloride (DAPI). The coverslips were mounted on glass slides using Moviol (Calbiochem, Nottingham, UK) and observed by fluorescence microscopy. In addition, the assessment of cell death when macrophage and SHSY5Y cells coincubated with PTX3 was performed as follows. First, the SH-SY5Y cells were labeled with PKH-67 green fluorescent cell linker dye (Sigma, St. Louis, MO, USA). Viable SH-SY5Y cells ( $5 \times 10^5$ ) and monocyte-derived macrophages ( $5 \times 10^5$ /well) were washed with PBS 3 times. SH-SY5Y cells were resuspended in serum free RPMI medium to induce cell death before being added into macrophage coculture. Cell interaction was allowed for 24 hours at 37 °C in 5% CO<sub>2</sub>. Cell death was detected by staining with propidium iodide and fluorescence microscopy or quantitative analysis by flow cytometry.

#### 2.14. Conditioned medium concentration and enzyme-linked immunosorbent assay (ELISA)

Medium was collected after 24 hours of culture with ZnSO<sub>4</sub> (100 μM) from various stable U373MG cell lines containing inducible CEBPD expression vector and then concentrated from 10 mL into 200 μL volume by Amicon Ultra-15 centrifugal filter (Millipore, Billerica, MA, USA) according to manufacturer's instructions. Expression of PTX3 in supernatants was quantified with a commercially available ELISA, according to manufacturer's instructions (Quantikine® ELISA kit, R&D, Minneapolis, MN, USA).

#### 2.15. Immunohistochemistry

Brain tissue dissections were postfixed in 4% buffered paraformaldehyde for 24–36 hours, cryoprotected, sectioned at 10 μm on a freezing microtome, and stored at –20 °C in 33% glycerin, 33% glycerol, 33% phosphate buffer (pH 7.4) solutions. After blocking in 3% bovine serum albumin, the sections were incubated overnight in first antibody. Detection of immunoreactivity employed Vectastain (VECTOR, Burlingame, CA, USA) kits with a diaminobenzidine label.

### 3. Results

Elevated CEBPD expression was reported in astrocytes of AD patients (Li et al., 2004). Many regulatory motifs of transcription factors are conserved between the promoters of the human *CEBPD* and mouse *Cebpd* genes (Wang et al., 2005). Therefore, we analyzed the transgenic *App* mouse model for AD to see if it recapitulates induced CEBPD expression. First, we confirmed the appearance of Aβ-plaques in the mouse brains (Fig. 1A). Next, Western analysis showed that *Cebpd* protein was specifically induced in the brains of *App* transgenic mice (Fig. 1B), demonstrating a causal relationship of Aβ and *Cebpd* expression in vivo. Moreover, treatment with Aβ, IL-1β, or TNF-α could activate *Cebpd* transcripts in enriched mouse glial cell cultures consisting primarily of astrocytes (Fig. 1B, right panel). These data imply that the induction of Aβ-induced *Cebpd* could occur through the actions of IL-1β and TNF-α. Furthermore, *CEBPD* expression was examined in human astrocytes (U373MG) and monocytes (THP-1) after treatment with IL-1β or TNF-α. As shown in Fig. 1C, both cytokines could increase *CEBPD* transcript levels in U373MG and THP-1 cells. These data show that factors associated with AD induce *CEBPD* expression in mouse and human astrocytes in vitro.

To identify the spectrum of genes controlled by CEBPD in astrocytes, U373MG cells stably transfected with a zinc-inducible CEBPD expression construct were generated for global gene expression profiling. In this system, CEBPD was induced approximately 6-fold by 8 hours of zinc treatment (Fig. 2A, left panel) at which point total RNA was harvested and microarray profiling analysis was performed. Among the genes screened, expression of 430 genes was modulated by CEBPD with statistical significance (Fig. 2A, right panel). A total of 236 genes were induced while 194 genes were inhibited by CEBPD. Table 1 shows a selection of CEBPD-responsive genes in 5 categories related to inflammation-related biology according to the Ingenuity pathway analysis program (Table 1). To verify the microarray results, several genes were analyzed by RT-PCR, which confirmed induction or



repression by CEBPD as predicted by the microarray (Fig. 2B). Next, we examined whether these CEBPD regulated genes were also responsive to TNF- $\alpha$  or IL-1 $\beta$ . RT-PCR analysis of U373MG cells revealed that CEBPD-induced genes identified by microarray, were also activated by TNF- $\alpha$  or IL-1 $\beta$  (Fig. 2C). This result raises the possibility that CEBPD mediates the IL-1 $\beta$  and TNF- $\alpha$ -induced expression of these genes in astrocytes of AD.

Because phagocytosis is deficient in most AD patients (Fiala et al., 2007), we decided to test whether CEBPD-regulated secreted proteins may function in the regulation of phagocytosis. To this end, we assessed phagocytosis of apoptotic SH-SY5Y neuronal cells by THP-1 derived macrophages (Fig. 3A and B). When macrophages were incubated with conditioned medium from U373MG cells expressing CEBPD (+ZnSO<sub>4</sub>), the phagocytosis rate was significantly attenuated compared with cells exposed to control conditioned medium (Fig. 3C). Similar results were obtained when the experiment was performed with apoptotic primary mouse neurons (Fig. 3D). These results show that CEBPD can induce secreted factors in astrocytes, which attenuate phagocytosis of dead neurons by activated macrophages. Hence, overexpression of CEBPD may result in the accumulation of dead cells and consequently enhanced apoptosis of neurons in neurodegenerative diseases.

The microarray data indicated that CEBPD could induce expression of *PTX3* (Fig. 2B and C, and Supplemental Fig. 1). *PTX3* is induced by inflammatory signals and can inhibit the phagocytosis of apoptotic cells by dendritic cells and macrophages (see Introduction). Therefore, we asked if *PTX3* was the CEBPD-induced secreted factor that attenuated phagocytosis. We first examined whether mouse *PTX3* (*Ptx3*) expression can be activated by A $\beta$ , TNF- $\alpha$ , or IL-1 $\beta$  in primary glial cells. As shown in Fig. 4A, *Ptx3* transcripts were induced by all of these stimuli. Furthermore, ectopic CEBPD induced *PTX3* mRNA levels in human U373MG and THP-1 cells (Fig. 4B), indicating that CEBPD-regulated *PTX3* expression is not cell type- or species-specific. To verify if endogenous CEBPD can mediate proinflammatory factor-induced *PTX3* expression, we depleted CEBPD by small interfering RNA (siRNA) (siD) in U373MG cells, which attenuated the TNF- $\alpha$ -induced *PTX3* transcript levels in a dose-dependent manner (Fig. 4C). Furthermore, *Ptx3* transcription was also reduced in *Cebpd*-deficient MEFs treated with TNF- $\alpha$  or IL-1 $\beta$  compared with wild-type MEFs (Fig. 4D). Lastly, we show that immunoassays detected *PTX3* protein specifically in media of U373MG cells with Zn-induced CEBPD expression (Fig. 4E). Collectively, we conclude from these results that CEBPD is an upstream activator of *PTX3* expression.

To determine if CEBPD activates *PTX3* transcription through its promoter, various 5'-flanking regions of the *PTX3* gene were cloned in front of a luciferase reporter (Fig. 5A, left panel). Cotransfection of CEBPD, in combination with WT-1200 or WT-473 but not WT-44, induced a 2.5-fold increase in reporter activity. This result suggested that sequences between positions -473 and -44 of the *PTX3* gene promoter were essential for CEBPD action. Reporter activity from the WT-473 construct was also induced by e IL-1 $\beta$  or TNF- $\alpha$ , and attenuated by a dominant negative mutant of CEBPD (Fig. 5B). These results suggest that endogenous CEBPD mediates at least in part IL-1 $\beta$ - and TNF- $\alpha$ -induced *PTX3* promoter activity.

The 5 members of the CCAAT/enhancer binding protein (CEBP) family all bind to the same DNA sequences by virtue of a highly conserved DNA binding domain (Osada et al., 1996). Although CEBP-binding motifs can be predicted by several online programs, such as TFSEARCH ([www.cbrc.jp/research/db/TFSEARCH.html](http://www.cbrc.jp/research/db/TFSEARCH.html)), there is no program for the prediction of specifically CEBPD binding. However, Osada et al. characterized that each protein displays certain sequence preferences at least in vitro (Osada et al., 1996). Using the information in their report, we created an internet program named “Prediction of CEBPD-Binding Motifs” (PCDBM; <http://web.ibbt.ncku.edu.tw:8080/wjmlab/PCDBM>; Supplemental Fig. 2). This program allows the user to obtain the 5=-flanking region of the gene of interest and identify putative CEBPD-binding motifs. The PCDBM and TFSEARCH programs predicted the same 5 putative CEBPD-binding elements in the *PTX3* promoter (Fig. 5A), while TFSEARCH predicted 1 additional site (site 4). Binding of CEBPD to these sites was verified by electrophoretic mobility shift assay (EMSA). According to PCDBM sites 5 (score = 92) and 1 (score = 100) possessed the highest CEBPD-binding activities, whereas TFSEARCH gave the highest scores to sites 5 (score = 86), 6 (score = 88), and 1 (score = 88). The electrophoretic mobility shift assay (EMSA) revealed a better correlation of binding activity with the prediction of PCDBM (Fig. 5C). Therefore, we suggest that PCDBM could be a reliable program for predicting specific CEBPD-binding motifs. To further assess if sites 1 and 5 are critical for CEBPD-mediated activation of the *PTX3* gene, we mutated these sites within the reporter constructs. The *PTX3* promoters containing a point mutation at sites 1 (M1), 5 (M5) or both (M1/M5) were cotransfected with the CEBPD expression vector. Attenuated reporter activities were observed in the cotransfectants with M1 or M5 reporters, and the M1/M5 reporter did not respond at all to CEBPD (Fig. 5D).

To examine whether CEBPD binds directly to the endogenous *PTX3* promoter, we performed an in vivo DNA binding assay. In both THP-1 and U373MG cells, IL-1 $\beta$  and TNF- $\alpha$  stimulated the association of endogenous CEBPD with the *PTX3* gene promoter (Fig. 6). These results demonstrate that proinflammatory factor-induced CEBPD binds to the *PTX3* promoter to activate gene transcription.

Extensive evidence suggests that amyloid deposition provokes a microglial-mediated inflammatory response that significantly contributes to cell loss and cognitive decline that is characteristic of AD (see Introduction). Our aforementioned results show that the conditioned medium of CEBPD-expressing astrocytes can inhibit phagocytosis of dead neurons by macrophages (Fig. 3A and B). Moreover, we have demonstrated that CEBPD induces transcription of *PTX3*, an extracellular protein involved in the regulation of phagocytosis in the inflammatory response (Supplemental Fig. 1). To probe the direct effect of *PTX3* on phagocytosis, increasing amounts of recombinant *PTX3* were added to macrophages. Indeed, *PTX3* could attenuate the efficiency by which macrophages phagocytosed apoptotic SH-SY5Y cells (Fig. 7A). To investigate the consequence of the accumulation of dying neuron cells, we incubated macrophages with serum-starved SH-SY5Y cells. The dying SHSY5Y cells were then further examined for apoptosis by PI staining. An enhancement of the accumulation of PI-positive SH-SY5Y cells was observed in the presence of *PTX3* in a dose-dependent manner (Fig. 7B). These results suggest that *PTX3* secretion may exacerbate neuronal cell death by blocking phagocytosis of dead neurons by macrophages in inflamed areas.

## 4. Discussion

Alzheimer's disease and other neurodegenerative disorders are in part the result of the interplay between neurons, glia, and inflammatory cells. However, much is to be learned about how these different cell types contribute to the disease phenotype. In this report we have shown that  $A\beta$  induced CEBPD expression in astrocytes and microglial cells *in vitro* as well as in brains of *App* transgenic mice *in vivo*. Gene expression analyses revealed that CEBPD regulates secreted factors with implications for AD such as TNF-alpha-induced protein 6 (TNFAIP6), CXC (C-X-C motif) chemokine receptor 4 (CXCR4) and PTX3 in U373MG astrocytes. Interestingly, the conditional medium of CEBPD expressing U373MG cells attenuated macrophage-mediated phagocytosis of dead neurons, and this activity was replicated by purified PTX3. This report identified PTX3 as a novel CEBPD target. The production of PTX3 has been demonstrated in smooth muscle cells, adipocytes, mononuclear phagocytes, and dendritic cells (Abderrahim-Ferkoune et al., 2004; Alles et al., 1994; Doni et al., 2003; Introna et al., 1996; Klouche et al., 2004), and all these cell types can also express CEBPD (Lai et al., 2008; Sekine et al., 2002; Serio et al., 2005). Also the NF- $\kappa$ B pathway activates transcription of the *PTX3* gene (Basile et al., 1997). Notably, CEBPD itself is a target gene of NF- $\kappa$ B and can amplify NF- $\kappa$ B signaling (Litvak et al., 2009). Hence, NF- $\kappa$ B and CEBPD may cooperate in activation of *PTX3* transcription in different cell types. These data suggest that CEBPD, within a loop of proinflammatory signals, and its target PTX3 are at least in part responsible for the previously unexplained observation that phagocytosis activity is low in AD patients (Fiala et al., 2007).

An accumulation of activated glial cells, particularly microglia and astrocytes, has been observed in the same areas as amyloid plaques. In addition, astrocytes also extensively interact with neurons and provide the structure and metabolic support for the homeostasis and the maintenance of normality of brain neurons. Moreover, astrocyte reactivity (i.e., activation) and associated neuroinflammation are increasingly thought to contribute to neurodegenerative diseases (see Introduction). While induced expression of C/EBP genes at sites of neuroinflammation or neural damage has been described before (Perez-Capote et al., 2006), the identification and function of their target genes, especially for CEBPD, have rarely been discussed. Here, a global profiling of CEBPD-regulated genes in astrocytes is provided (Table 1 and Supplemental Table 2), which includes several known CEBPD or C/EBP target genes, such as *PDGFRA*, *CEBPA*, *CEBPE*, *MMP3*, *ID2*, *MT1s*, *GABRE*, *RGS2*, *BCL2L1*, and *CTGF* (Cao et al., 1991; Connors et al., 2009; Fukuoka et al., 1999; Karaya et al., 2005; Sato et al., 2006; Thangaraju et al., 2005) as well as novel genes. Several target genes, such as *ID2*, *ALB*, *DGNF*, and *CTGF*, are suggested to be connected with AD. Several candidate target genes, such as *FGF4*, *THBS*, *MMP1*, *MMP10*, and *MMP3*, are known to participate in the inflammation process but have not yet been reported in AD. Progressive memory deficits, cognitive impairment, and personality changes are also characteristic of AD patients. Interestingly, loss of *Cebpd* improved specific memory functions in mice (Sterneck et al., 1998). While it remains to be determined if this is due to a role of *Cebpd* in neurons or glia/astrocytes, the observation is in line with overexpression of CEBPD possibly contributing to the AD phenotype.

The profiling of CEBPD-regulated gene expression in astrocytes may also provide interesting candidates for regulating cell survival and the neuron-glia cell interactions. CEBPD decreased expressions of *GNDF*, *THBS*, *AKT1*, and *BCL2L1*, but activate expressions of *BCL2L11* and *casP8* (Table 1 and Supplemental Table 2). GDNF and THBS were suggested to protect neuron cells and suppress inflammation (Ghribi et al., 2001; Oh et al., 2008). AKT1 and BCL2L1 (BCL-xL) were implicated in the maintenance of astrocytes, and also in protecting brain neurons (Di Iorio et al., 2004; Xu et al., 1999). BCL2L11 (Bim) and CASP8 (caspase 8) are suggested to participate in the activation of astrocytes (Falsig et al., 2004; Lee et al., 2009). Hence these expression changes are mostly in line with a role of CEBPD in astrocyte activation and neuronal cell death. However, the functional relevance of these genes in AD and as CEBPD targets remains to be determined. Furthermore, it will be interesting to investigate how posttranslational modification, which play a critical role in CEBPD's precise functions (Lai et al., 2008; Wang et al., 2006, 2008), modulate expression of these genes.

In addition to  $A\beta$ , TNF- $\alpha$ , and IL-1 $\beta$ , which activate CEBPD transcription in astrocytes as reported here, CEBPD is also induced by bacterial lipopolysaccharide (LPS) in various cell types (Liu et al., 2007; Rabek et al., 1998). Increasing evidence shows that bacteria and their persistent remnants may play a role in the accumulation of inflammatory effects and amyloid plaques in AD (Miklossy, 2008). Baruah et al. suggested that PTX3 confers immediate protection when acute inflammation and extensive cell death coexist, while limiting the onset and possibly the maintenance of autoimmune phenomena (Baruah et al., 2006; Manfredi et al., 2005). An accumulation of apoptotic cell remnants can challenge the immune system and trigger proinflammatory responses and eventually chronic autoimmune diseases such as systemic lupus erythematosus (Gaipl et al., 2004). Here, we demonstrated that PTX3 can inhibit the engulfment of dead neurons by differentiated THP-1 macrophages, and enhance the accumulation of dying SHSY5Y cells. The net effect of PTX3 may be in the accumulation of dead neurons that were damaged by inflammation in brain areas. Therefore, we suggest that the induction of CEBPD can enhance the accumulation of apoptotic cells, which amplifies the inflammatory response through PTX3 in AD, or other inflammation-related diseases. We suggest that detection of PTX3 in cerebrospinal fluid could be assessed as a diagnostic tool for AD progression.

## Supplementary Material

Refer to Web version on PubMed Central for supplementary material.

## Acknowledgements

This work was supported in part by NSC grant 96-2320-B-006-044-MY2 and by NCKU landmark grant C007 (Taiwan). Fund for Open Access publication was provided by the NCKU landmark grant C007. We thank Ms. Christine C. Hsieh for her critical review of the manuscript.

## References

- Abderrahim-Ferkoune A, Bezy O, Astri-Roques S, Elabd C, Ailhaud G, Amri EZ, 2004 Transdifferentiation of preadipose cells into smooth muscle-like cells: role of aortic carboxypeptidase-like protein. *Exp. Cell Res* 293, 219–228. [PubMed: 14729459]

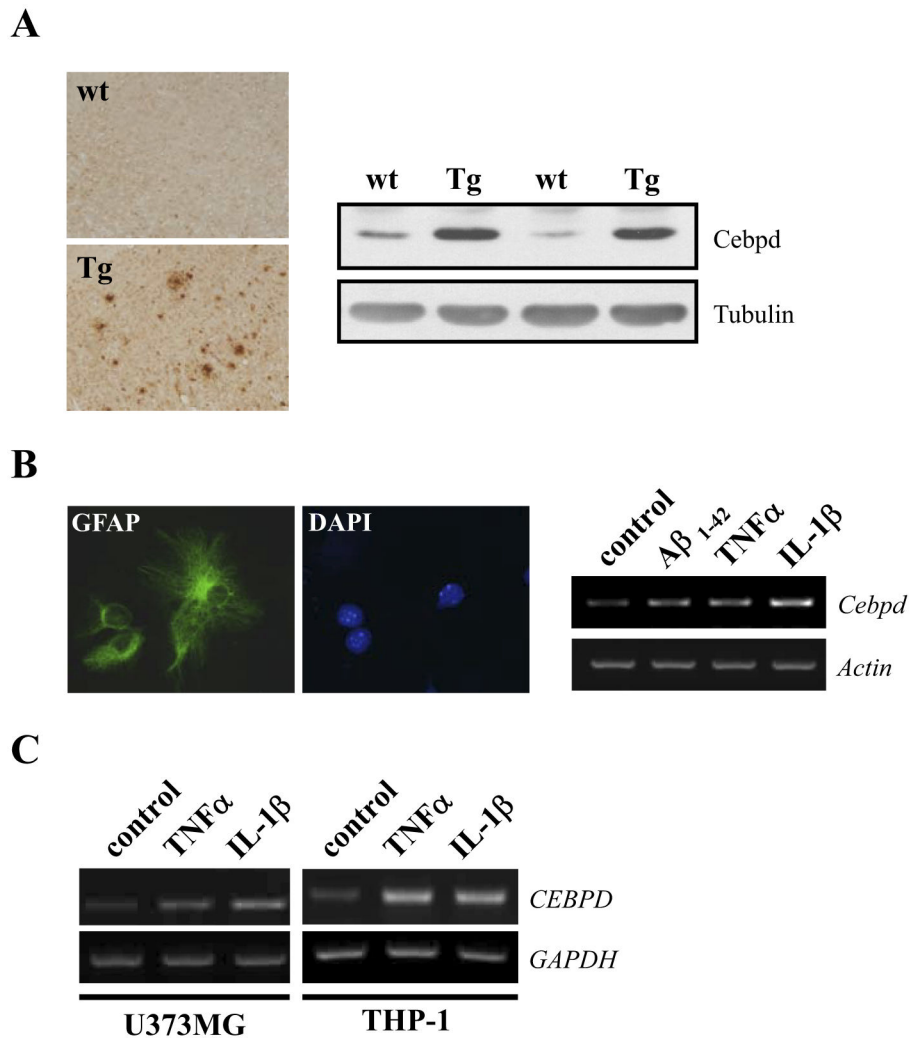
- Alles VV, Bottazzi B, Peri G, Golay J, Introna M, Mantovani A, 1994 Inducible expression of PTX3, a new member of the pentraxin family, in human mononuclear phagocytes. *Blood* 84, 3483–3493. [PubMed: 7949102]
- Altmeyer A, Klampfer L, Goodman AR, Vilcek J, 1995 Promoter structure and transcriptional activation of the murine TSG-14 gene encoding a tumor necrosis factor/interleukin-1-inducible pentraxin protein. *J. Biol. Chem* 270, 25584–25590. [PubMed: 7592730]
- Baruah P, Propato A, Dumitriu IE, Rovere-Querini P, Russo V, Fontana R, Accapezzato D, Peri G, Mantovani A, Barnaba V, Manfredi AA, 2006 The pattern recognition receptor PTX3 is recruited at the synapse between dying and dendritic cells, and edits the cross-presentation of self, viral, and tumor antigens. *Blood* 107, 151–158. [PubMed: 16166594]
- Basile A, Sica A, d'Aniello E, Breviario F, Garrido G, Castellano M, Mantovani A, Introna M, 1997 Characterization of the promoter for the human long pentraxin PTX3. Role of NF-kappaB in tumor necrosis factor-alpha and interleukin-1beta regulation. *J. Biol. Chem* 272, 8172–8178. [PubMed: 9079634]
- Bonifati DM, Kishore U, 2007 Role of complement in neurodegeneration and neuroinflammation. *Mol. Immunol* 44, 999–1010. [PubMed: 16698083]
- Bottazzi B, Bastone A, Doni A, Garlanda C, Valentino S, Deban L, Maina V, Cotena A, Moalli F, Vago L, Salustri A, Romani L, Mantovani A, 2006 The long pentraxin PTX3 as a link among innate immunity, inflammation, and female fertility. *J. Leukoc. Biol* 79, 909–912. [PubMed: 16478917]
- Breviario F, d'Aniello EM, Golay J, Peri G, Bottazzi B, Bairoch A, Saccone S, Marzella R, Predazzi V, Rocchi M, 1992 Interleukin-1-inducible genes in endothelial cells. Cloning of a new gene related to C-reactive protein and serum amyloid P component. *J. Biol. Chem* 267, 22190–22197. [PubMed: 1429570]
- Cao Z, Umek RM, McKnight SL, 1991 Regulated expression of three C/EBP isoforms during adipose conversion of 3T3-L1 cells. *Genes Dev* 5, 1538–1552. [PubMed: 1840554]
- Cardinaux JR, Allaman I, Magistretti PJ, 2000 Pro-inflammatory cytokines induce the transcription factors C/EBPbeta and C/EBPdelta in astrocytes. *Glia* 29, 91–97. [PubMed: 10594926]
- Castelo-Branco G, Wagner J, Rodriguez FJ, Kele J, Sousa K, Rawal N, Pasolli HA, Fuchs E, Kitajewski J, Arenas E, 2003 Differential regulation of midbrain dopaminergic neuron development by Wnt-1, Wnt-3a, and Wnt-5a. *Proc. Natl. Acad. Sci. U. S. A* 100, 12747–12752. [PubMed: 14557550]
- Cole DS, Hughes TR, Gasque P, Morgan BP, 2006 Complement regulator loss on apoptotic neuronal cells causes increased complement activation and promotes both phagocytosis and cell lysis. *Mol. Immunol* 43, 1953–1964. [PubMed: 16406094]
- Connors SK, Balusu R, Kundu CN, Jaiswal AS, Gairola CG, Narayan S, 2009 C/EBPbeta-mediated transcriptional regulation of *bcl-xl* gene expression in human breast epithelial cells in response to cigarette smoke condensate. *Oncogene* 28, 921–932. [PubMed: 19043455]
- Di Iorio P, Ballerini P, Traversa U, Nicoletti F, D'Alimonte I, Kleywegt S, Werstiuk ES, Rathbone MP, Caciagli F, Ciccarelli R, 2004 The antiapoptotic effect of guanosine is mediated by the activation of the PI 3-kinase/AKT/PKB pathway in cultured rat astrocytes. *Glia* 46, 356–368. [PubMed: 15095366]
- Doni A, Peri G, Chieppa M, Allavena P, Pasqualini F, Vago L, Romani L, Garlanda C, Mantovani A, 2003 Production of the soluble pattern recognition receptor PTX3 by myeloid, but not plasmacytoid, dendritic cells. *Eur. J. Immunol* 33, 2886–2893. [PubMed: 14515272]
- Falsig J, Latta M, Leist M, 2004 Defined inflammatory states in astrocyte cultures: correlation with susceptibility towards CD95-driven apoptosis. *J. Neurochem* 88, 181–193. [PubMed: 14675162]
- Fiala M, Cribbs DH, Rosenthal M, Bernard G, 2007 Phagocytosis of amyloid-beta and inflammation: two faces of innate immunity in Alzheimer's disease. *J. Alzheimers Dis* 11, 457–463. [PubMed: 17656824]
- Fukuoka T, Kitami Y, Okura T, Hiwada K, 1999 Transcriptional regulation of the platelet-derived growth factor alpha receptor gene via CCAAT/enhancer-binding protein-delta in vascular smooth muscle cells. *J. Biol. Chem* 274, 25576–25582. [PubMed: 10464291]
- Gaipl US, Franz S, Voll RE, Sheriff A, Kalden JR, Herrmann M, 2004 Defects in the disposal of dying cells lead to autoimmunity. *Curr. Rheumatol. Rep* 6, 401–407. [PubMed: 15527698]

- Gao H, Bryzgalova G, Hedman E, Khan A, Efendic S, Gustafsson JA, Dahlman-Wright K, 2006 Long-term administration of estradiol decreases expression of hepatic lipogenic genes and improves insulin sensitivity in ob/ob mice: a possible mechanism is through direct regulation of signal transducer and activator of transcription. 3. *Mol. Endocrinol* 20, 1287–1299. [PubMed: 16627594]
- Ghribi O, Herman MM, Forbes MS, DeWitt DA, Savory J, 2001 GDNF protects against aluminum-induced apoptosis in rabbits by up-regulating Bcl-2 and Bcl-XL and inhibiting mitochondrial Bax trans-location. *Neurobiol. Dis* 8, 764–773. [PubMed: 11592846]
- Giulian D, Haverkamp LJ, Li J, Karshin WL, Yu J, Tom D, Li X, Kirkpatrick JB, 1995 Senile plaques stimulate microglia to release a neurotoxin found in Alzheimer brain. *Neurochem. Int* 27, 119–137. [PubMed: 7655344]
- Glass CK, Saijo K, Winner B, Marchetto MC, Gage FH, 2010 Mechanisms underlying inflammation in neurodegeneration. *Cell* 140, 918–934. [PubMed: 20303880]
- Introna M, Alles VV, Castellano M, Picardi G, De Gioia L, Bottazzai B, Peri G, Breviario F, Salmona M, De Gregorio L, Dragani TA, Srinivasan N, Blundell TL, Hamilton TA, Mantovani A, 1996 Cloning of mouse ptx3, a new member of the pentraxin gene family expressed at extrahepatic sites. *Blood* 87, 1862–1872. [PubMed: 8634434]
- Itagaki S, McGeer PL, Akiyama H, Zhu S, Selkoe D, 1989 Relationship of microglia and astrocytes to amyloid deposits of Alzheimer disease. *J. Neuroimmunol* 24, 173–182. [PubMed: 2808689]
- Karaya K, Mori S, Kimoto H, Shima Y, Tsuji Y, Kurooka H, Akira S, Yokota Y, 2005 Regulation of Id2 expression by CCAAT/enhancer binding protein beta. *Nucleic Acids Res* 33, 1924–1934. [PubMed: 15809228]
- Clouche M, Peri G, Knabbe C, Eckstein HH, Schmid FX, Schmitz G, Mantovani A, 2004 Modified atherogenic lipoproteins induce expression of pentraxin-3 by human vascular smooth muscle cells. *Atherosclerosis* 175, 221–228. [PubMed: 15262177]
- Lai PH, Wang WL, Ko CY, Lee YC, Yang WM, Shen TW, Chang WC, Wang JM, 2008 HDAC1/HDAC3 modulates PPAR $\gamma$ 2 transcription through the sumoylated CEBPD in hepatic lipogenesis. *Biochim. Biophys. Acta* 1783, 1803–1814. [PubMed: 18619497]
- Lee S, Park JY, Lee WH, Kim H, Park HC, Mori K, Suk K, 2009 Lipocalin-2 is an autocrine mediator of reactive astrocytosis. *J. Neurosci* 29, 234–249. [PubMed: 19129400]
- Lee SC, Liu W, Brosnan CF, Dickson DW, 1994 GM-CSF promotes proliferation of human fetal and adult microglia in primary cultures. *Glia* 12, 309–318. [PubMed: 7890333]
- Li R, Strohmeyer R, Liang Z, Lue LF, Rogers J, 2004 CCAAT/enhancer binding protein delta (C/EBPdelta) expression and elevation in Alzheimer's disease. *Neurobiol. Aging* 25, 991–999. [PubMed: 15212823]
- Litvak V, Ramsey SA, Rust AG, Zak DE, Kennedy KA, Lampano AE, Nykter M, Shmulevich I, Aderem A, 2009 Function of C/EBPdelta in a regulatory circuit that discriminates between transient and persistent TLR4-induced signals. *Nat. Immunol* 10, 437–443. [PubMed: 19270711]
- Liu YW, Chen CC, Wang JM, Chang WC, Huang YC, Chung SY, Chen BK, Hung JJ, 2007 Role of transcriptional factors Sp1, c-Rel, and c-Jun in LPS-induced C/EBPdelta gene expression of mouse macrophages. *Cell. Mol. Life Sci* 64, 3282–3294. [PubMed: 17965828]
- Manfredi AA, Sabbadini MG, Rovere-Querini P, 2005 Dendritic cells and the shadow line between autoimmunity and disease. *Arthritis Rheum* 52, 11–15. [PubMed: 15641071]
- Mantovani A, Garlanda C, Bottazzi B, 2003 Pentraxin 3, a non-redundant soluble pattern recognition receptor involved in innate immunity. *Vaccine* 21 suppl 2, S43–S47. [PubMed: 12763682]
- Martin LJ, Pardo CA, Cork LC, Price DL, 1994 Synaptic pathology and glial responses to neuronal injury precede the formation of senile plaques and amyloid deposits in the aging cerebral cortex. *Am. J. Pathol* 145, 1358–1381. [PubMed: 7992840]
- McGeer PL, McGeer EG, 1995 The inflammatory response system of brain: implications for therapy of Alzheimer and other neurodegenerative diseases. *Brain Res. Brain Res. Rev* 21, 195–218. [PubMed: 8866675]
- McGeer PL, McGeer EG, 2002 Local neuroinflammation and the progression of Alzheimer's disease. *J. Neurovirol* 8, 529–538. [PubMed: 12476347]
- Miklossy J, 2008 Chronic inflammation and amyloidogenesis in Alzheimer's disease – role of Spirochetes. *J. Alzheimers Dis* 13, 381–391. [PubMed: 18487847]

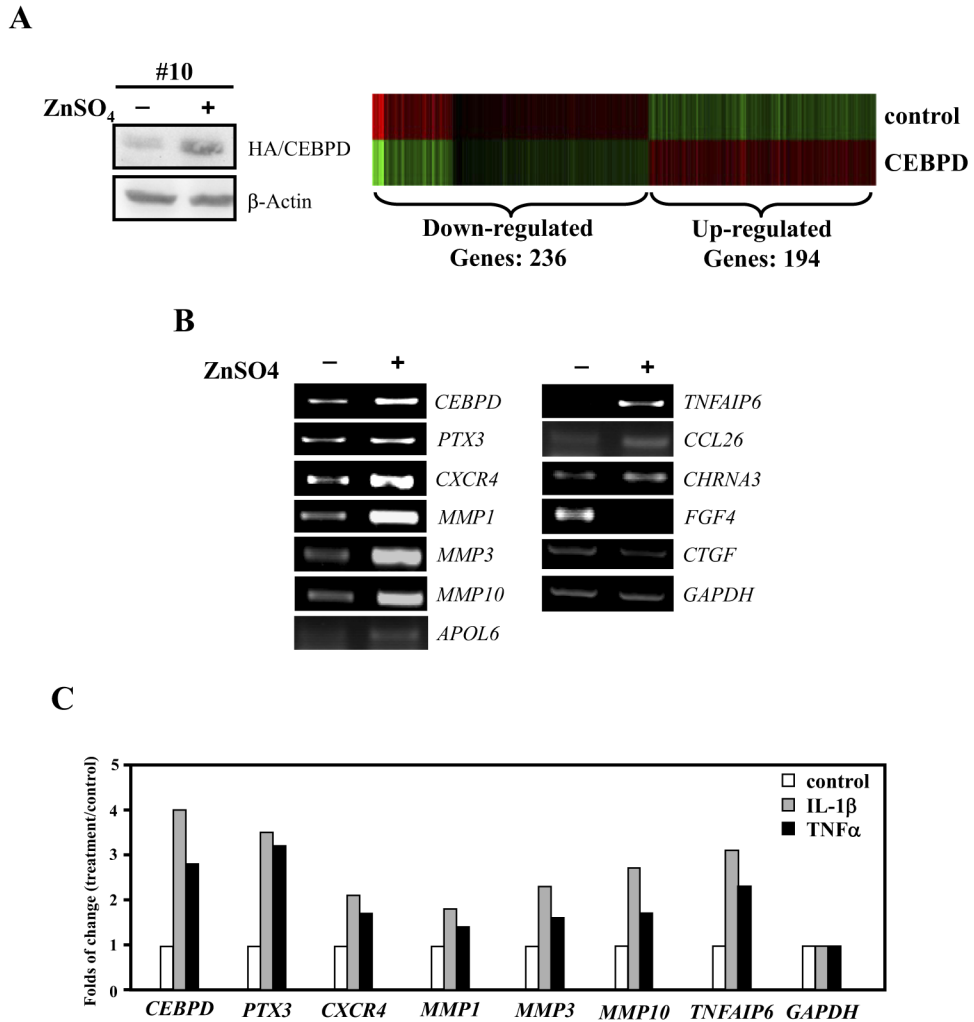
- Nishioka K, Ohshima S, Umeshita-Sasai M, Yamaguchi N, Mima T, Nomura S, Murata N, Shimizu M, Miyake T, Yoshizaki K, Suemura M, Kishimoto T, Saeki Y, 2000 Enhanced expression and DNA binding activity of two CCAAT/enhancer-binding protein iso-forms, C/EBPbeta and C/EBPdelta, in rheumatoid synovium. *Arthritis Rheum* 43, 1591–1596. [PubMed: 10902764]
- Oh JY, Kim MK, Shin MS, Lee HJ, Ko JH, Wee WR, Lee JH, 2008 The anti-inflammatory and anti-angiogenic role of mesenchymal stem cells in corneal wound healing following chemical injury. *Stem Cells* 26, 1047–1055. [PubMed: 18192235]
- Ortega-Hernandez OD, Bassi N, Shoenfeld Y, Anaya JM, 2009 The Long Pentraxin 3 and Its Role in Autoimmunity. *Semin. Arthritis Rheum* 39, 38–54. [PubMed: 18614204]
- Osada S, Yamamoto H, Nishihara T, Imagawa M, 1996 DNA binding specificity of the CCAAT/enhancer-binding protein transcription factor family. *J. Biol. Chem* 271, 3891–3896. [PubMed: 8632009]
- Perez-Capote K, Saura J, Serratos J, Sola C, 2006 Expression of C/EBPalpha and C/EBPbeta in glial cells in vitro after inducing glial activation by different stimuli. *Neurosci. Lett* 410, 25–30. [PubMed: 17070994]
- Qin H, Niyongere SA, Lee SJ, Baker BJ, Benveniste EN, 2008 Expression and functional significance of SOCS-1 and SOCS-3 in astrocytes. *J. Immunol* 181, 3167–3176. [PubMed: 18713987]
- Rabek JP, Scott S, Hsieh CC, Reisner PD, Papaconstantinou J, 1998 Regulation of LPS-mediated induction of C/EBP delta gene expression in livers of young and aged mice. *Biochim. Biophys. Acta* 1398, 137–147. [PubMed: 9689913]
- Ramji DP, Vitelli A, Tronche F, Cortese R, Ciliberto G, 1993 The two C/EBP isoforms, IL-6DBP/NF-IL6 and C/EBP delta/NF-IL6 beta, are induced by IL-6 to promote acute phase gene transcription via different mechanisms. *Nucleic Acids Res* 21, 289–294. [PubMed: 7680115]
- Sasaki A, Yamaguchi H, Ogawa A, Sugihara S, Nakazato Y, 1997 Microglial activation in early stages of amyloid beta protein deposition. *Acta Neuropathol* 94, 316–322. [PubMed: 9341931]
- Sato Y, Miyake K, Kaneoka H, Iijima S, 2006 Sumoylation of CCAAT/enhancer-binding protein alpha and its functional roles in hepatocyte differentiation. *J. Biol. Chem* 281, 21629–21639. [PubMed: 16735515]
- Sekine O, Nishio Y, Egawa K, Nakamura T, Maegawa H, Kashiwagi A, 2002 Insulin activates CCAAT/enhancer binding proteins and proinflammatory gene expression through the phosphatidylinositol 3-kinase pathway in vascular smooth muscle cells. *J. Biol. Chem* 277, 36631–36639. [PubMed: 12145301]
- Serio KJ, Reddy KV, Bigby TD, 2005 Lipopolysaccharide induces 5-lipoxygenase-activating protein gene expression in THP-1 cells via a NF-kappaB and C/EBP-mediated mechanism. *Am. J. Physiol. Cell Physiol* 288, C1125–C1133. [PubMed: 15625306]
- Staikos L, Malellari L, Chang SL, 2008 Lipopolysaccharide-induced pro-inflammatory cytokines in the brain of rats in the morphine-tolerant state. *J. Neuroimmune Pharmacol* 3, 236–240. [PubMed: 18584332]
- Sterneck E, Paylor R, Jackson-Lewis V, Libbey M, Przedborski S, Tessarollo L, Crawley JN, Johnson PF, 1998 Selectively enhanced contextual fear conditioning in mice lacking the transcriptional regulator CCAAT/enhancer binding protein delta. *Proc. Natl. Acad. Sci. U. S. A* 95, 10908–10913. [PubMed: 9724803]
- Streit WJ, Mrazek RE, Griffin WS, 2004 Microglia and neuroinflammation: a pathological perspective. *J. Neuroinflammation* 1, 14–17. [PubMed: 15285801]
- Takata Y, Kitami Y, Yang ZH, Nakamura M, Okura T, Hiwada K, 2002 Vascular inflammation is negatively autoregulated by interaction between CCAAT/enhancer-binding protein-delta and peroxisome proliferator-activated receptor-gamma. *Circ. Res* 91, 427–433. [PubMed: 12215492]
- Tessarollo L, 2001 Manipulating mouse embryonic stem cells. *Methods Mol. Biol* 158, 47–63. [PubMed: 11236671]
- Thangaraju M, Rudelius M, Bierie B, Raffeld M, Sharan S, Hennighausen L, Huang AM, Sterneck E, 2005 C/EBPdelta is a crucial regulator of pro-apoptotic gene expression during mammary gland involution. *Development* 132, 4675–4685. [PubMed: 16192306]

- Tsukada J, Saito K, Waterman WR, Webb AC, Auron PE, 1994 Transcription factors NF-IL6 and CREB recognize a common essential site in the human interleukin 1 beta gene. *Mol. Cell. Biol* 14, 7285–7297. [PubMed: 7935442]
- van Rossum AP, Fazzini F, Limburg PC, Manfredi AA, Rovere-Querini P, Mantovani A, Kallenberg CG, 2004 The prototypic tissue pentraxin PTX3, in contrast to the short pentraxin serum amyloid P, inhibits phagocytosis of late apoptotic neutrophils by macrophages. *Arthritis Rheum* 50, 2667–2674. [PubMed: 15334483]
- Wang JM, Tseng JT, Chang WC, 2005 Induction of human NFIL6beta by epidermal growth factor is mediated through the p38 signaling pathway and cAMP response element-binding protein activation in A431 cells. *Mol. Biol. Cell* 16, 3365–3376. [PubMed: 15901830]
- Wang JM, Ko CY, Chen LC, Wang WL, Chang WC, 2006 Functional role of NF-IL6beta and its sumoylation and acetylation modifications in promoter activation of cyclooxygenase 2 gene. *Nucleic Acids Res* 34, 217–231. [PubMed: 16397300]
- Wang WL, Lee YC, Yang WM, Chang WC, Wang JM, 2008 Sumoylation of LAP1 is involved in the HDAC4-mediated repression of COX-2 transcription. *Nucleic Acids Res* 36, 6066–6079. [PubMed: 18820298]
- Xu L, Lee JE, Giffard RG, 1999 Overexpression of bcl-2, bcl-XL or hsp70 in murine cortical astrocytes reduces injury of co-cultured neurons. *Neurosci. Lett* 277, 193–197. [PubMed: 10626846]

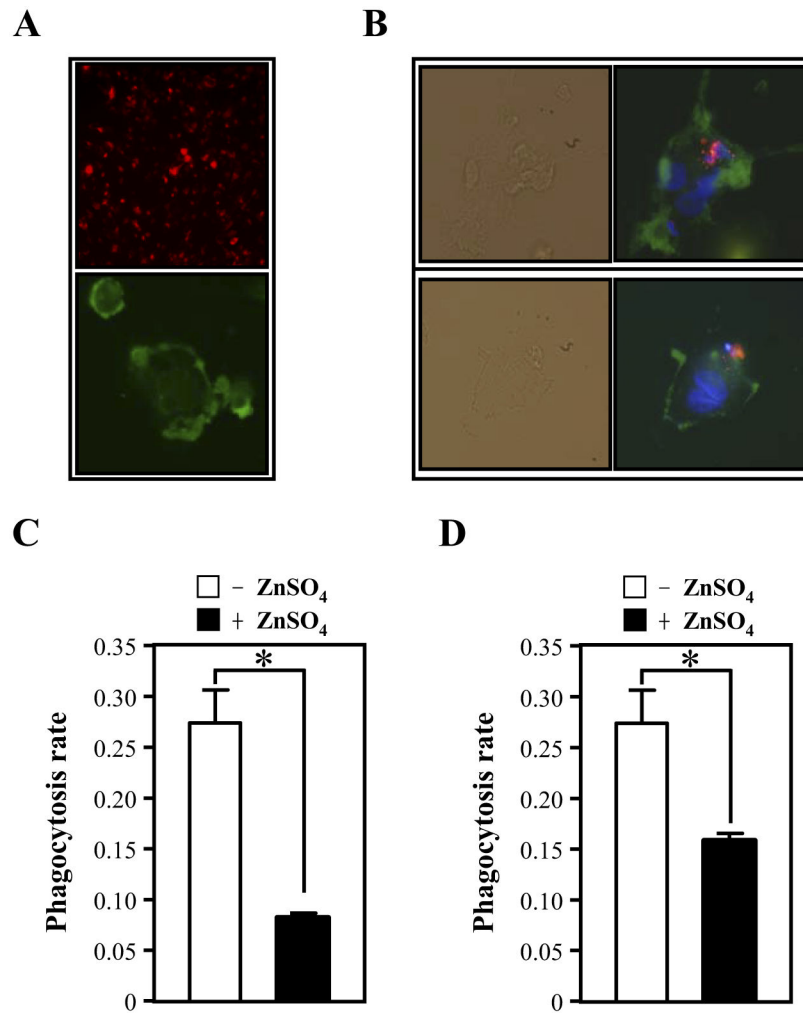




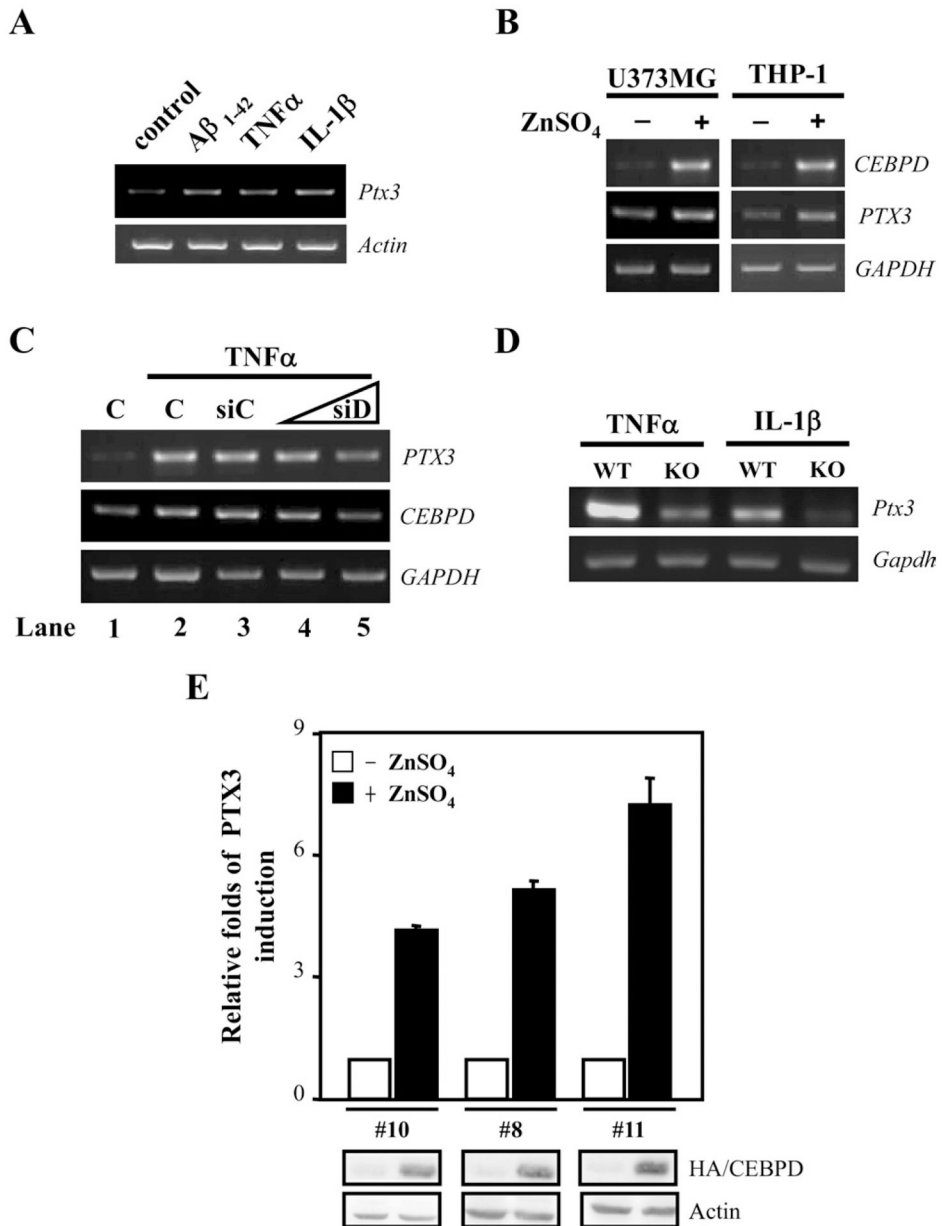
**Fig. 1.** CCAAT/enhancer binding protein delta (CEBPD) expression is induced in Alzheimer's disease (AD) models and by proinflammatory cytokines. (A) Sagittal sections and protein lysates of brain cortex were prepared from wild type (wt) and *APP* transgenic (Tg) mice, and subjected to immunohistochemistry with  $\beta$ -amyloid ( $A\beta$ ) antibody (left panel) or Western blot analysis with Cebpd antibody (right panel), respectively. (B) Enriched mouse primary glial cultures were derived from mice cerebral cortex and the glial cells were identified by immunofluorescence staining with GFAP antibody (left panel). Glial cells were then treated with 5  $\mu$ M  $A\beta_{1-42}$ , 20 ng/mL tumor necrosis factor alpha (TNF- $\alpha$ ), or 5 ng/mL interleukin (IL)-1 $\beta$  for 3 hours, and reverse transcription-polymerase chain reaction (RT-PCR) assay was performed to examine the expression of *Cebpd* mRNA (right panel). (C) U373MG and THP-1 cells were treated with 20 ng/mL TNF- $\alpha$  or 5 ng/ml IL-1 $\beta$  for 3 hours and *Cebpd* mRNA expression was examined by RT-PCR.



**Fig. 2.** Identification of CEBPD regulated genes in U373MG cells. (A) U373MG cells stably transfected with zinc-inducible CEBPD expression vector were exposed to 100  $\mu$ M ZnSO<sub>4</sub> for 8 hours and expression of HA-tagged CEBPD protein was analyzed by Western blotting (left panel). Clustering of microarray data from ribonucleic acid (RNA) of cells as shown in panel (A) identified significant gene expression clusters resulting from CEBPD overexpression (right panel). (B) Transcript levels of 11 differentially expressed genes, which code for membrane or secreted proteins, were assessed by reverse transcription-polymerase chain reaction (RT-PCR) analysis. *GAPDH* served as the loading control. (C) U373MG cells were treated with 20 ng/mL tumor necrosis factor alpha (TNF- $\alpha$ ) or 5 ng/ml interleukin (IL)-1 $\beta$  for 3 hours and RT-PCR of indicated genes was performed.

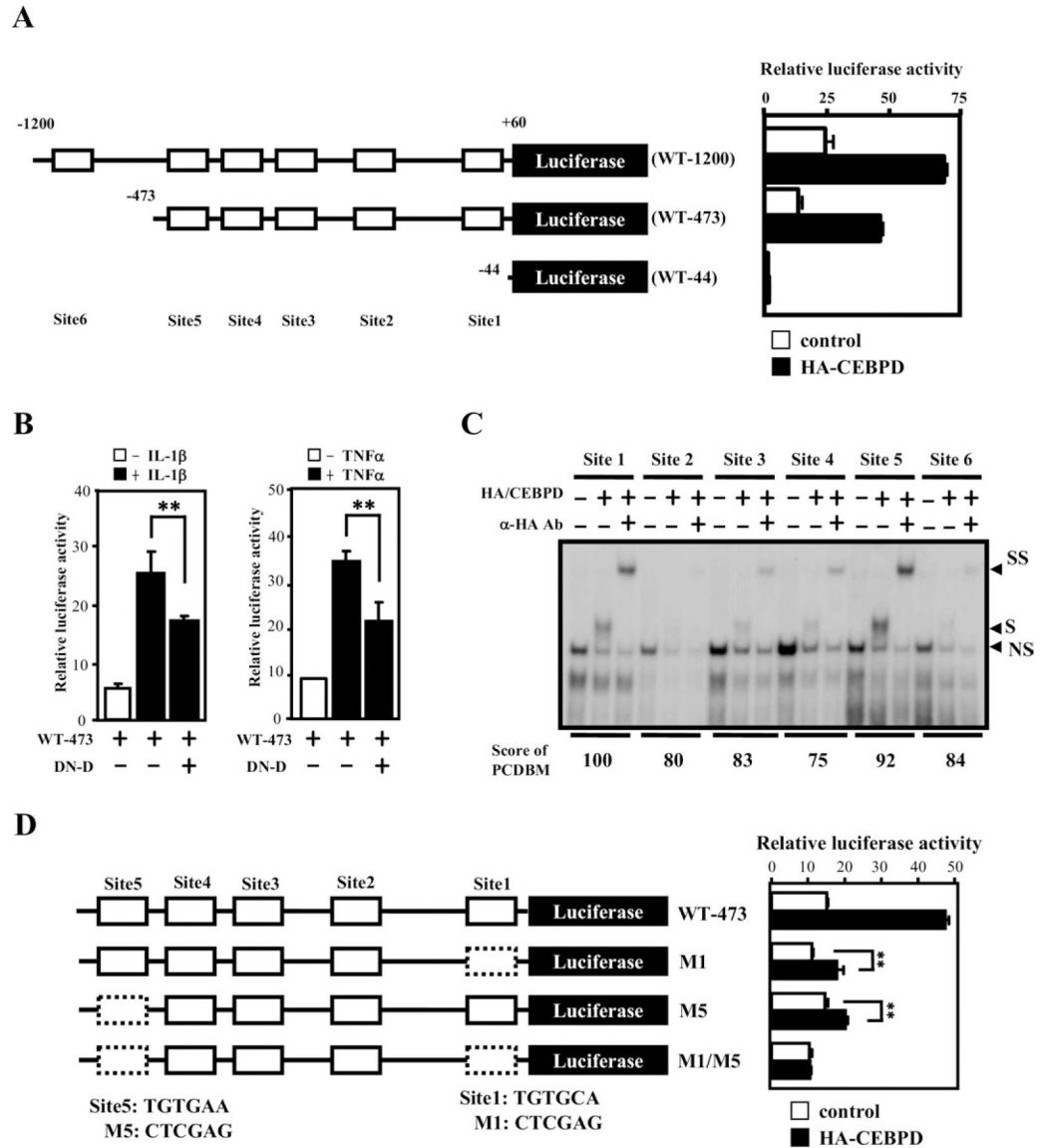


**Fig. 3.** Conditioned medium from U373MG cells overexpressing CEBPD inhibits the phagocytosis of apoptotic SH-SY5Y cells or primary neurons by macrophages. (A) SH-SY5Y cells were labeled with PKH26 red fluorescent membrane tracer (upper panel). THP-1 macrophages were stained with F4/80 (green) (bottom panel). (B) The SH-SY5Y cells (labeled with PKH26 red fluorescence) were induced to undergo apoptosis by irradiation and were then incubated with activated macrophages (labeled with F4/80 green fluorescence). The upper panel shows an apoptotic cell phagocytosed by a macrophage. The lower panel shows an apoptotic cell attached to the cell membrane of a macrophage. The bright field panel represents the phase contrast image. (C) The apoptotic SH-SY5Y cells or (D) apoptotic primary neurons were added to adherent monocyte-derived macrophages incubated with control ( $-ZnSO_4$ ) or CEBPD overexpressing ( $+ZnSO_4$ ) conditioned media for 30 minutes. Phagocytosis was quantified by flow cytometric analysis of fluorescent particles. The phagocytosis ratio was calculated by dividing the number of stained cells by the total number of macrophages (mean  $\pm$  SD,  $n = 3$ , \*  $p < 0.05$  by Student  $t$  test).



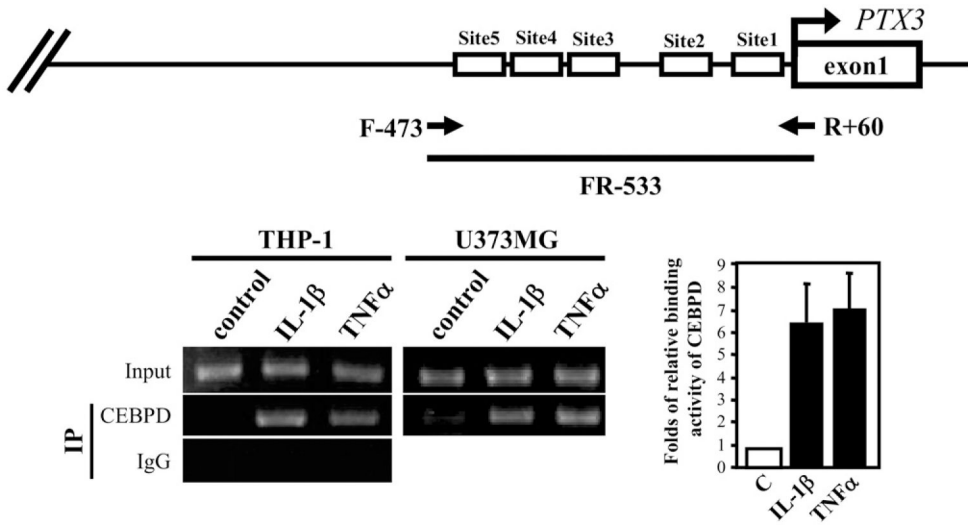
**Fig. 4.** Overexpression of CEBPD increases *PTX3* transcripts. (A) Primary glial cells were treated with 5  $\mu$ M  $\beta$ -amyloid ( $A\beta$ )<sub>1-42</sub>, 20 ng/mL tumor necrosis factor alpha (TNF- $\alpha$ ), or 5 ng/mL interleukin (IL)-1 $\beta$  for 3 hours, and reverse transcription-polymerase chain reaction (RT-PCR) assay was performed to examine the expression of *Ptx3* and *Actin* mRNAs. (B) U373MG and THP-1 cells were transiently transfected with the zinc-inducible CEBPD expression vector and then incubated in the presence or absence of 100  $\mu$ M ZnSO<sub>4</sub> in medium for 12 hours. RT-PCR assay was performed to examine the expression of *CEBPD*, *PTX3*, and *GAPDH* mRNAs. (C) U373MG cells were transiently transfected with 2  $\mu$ g of control knockdown vector (siC) or 1  $\mu$ g or 2  $\mu$ g of CEBPD knockdown vector (siD) and then treated with 20 ng/mL TNF- $\alpha$  for 6 hours. RT-PCR assay was performed to examine the

expression of *CEBPD*, *PTX3*, and *GAPDH* mRNAs. C, nontransfected. (D) *Ptx3* mRNA levels were assessed in wild type (WT) and *Cebpd* knockout (KO) MEFs by RT-PCR analysis. (E) The conditioned medium harvested from various U373MG stable clones bearing zinc-inducible HA/CEBPD expression vectors were analyzed by enzyme-linked immunosorbent assay (ELISA) to quantify PTX3 protein concentration. The fold induction over untreated cells is shown (mean  $\pm$  SD,  $n=3$ ). Western analysis of CEBPD expression is shown at the bottom.



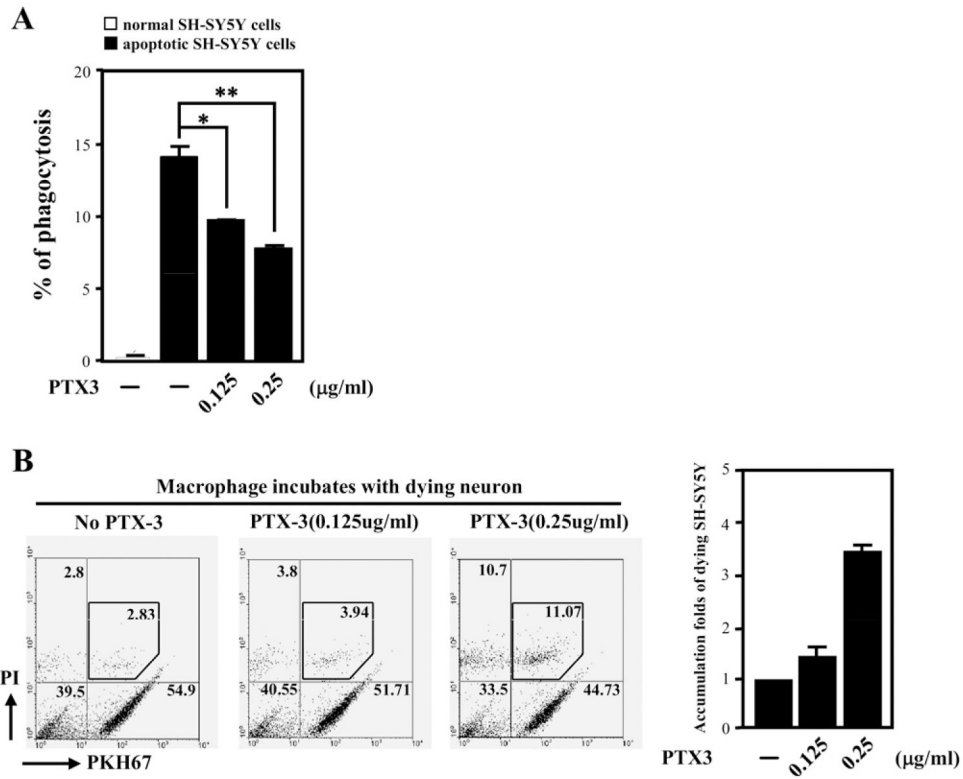
**Fig. 5.** CEBPD-binding motifs are important for CEBPD-induced *PTX3* reporter activity. (A) Schematic representation of reporter constructs with the human *PTX3* promoter (left panel). Numbers indicate the number of base pairs upstream (-) and downstream (+) of the *PTX3* translation start site. The approximate location of putative CEBPD-binding motifs (site 1–6) is indicated by open boxes. Luciferase activity from these reporter constructs in U373MG cells 12 hours after cotransfected with CEBPD expression or control vectors is shown on the right (mean  $\pm$  SD,  $n = 3$ ). (B) A dominant-negative CEBPD protein attenuates tumor necrosis factor alpha (TNF- $\alpha$ )- and interleukin (IL)-1 $\beta$ -activated *PTX3* reporter activities. The *PTX3* reporter, PTX3–473, was cotransfected with a dominant-negative CEBPD expression vector (DN-D) into U373MG cells. Lysates of the transfectants were harvested for luciferase assay 12 hours after transfection (mean  $\pm$  SD,  $n = 3$ , \*\*  $p < 0.01$  by Student  $t$  test). (C) CEBPD protein binds sites 1 and 5 with highest affinity. An electrophoretic

mobility shift assay was performed with  $^{32}\text{P}$ -labeled probes bearing the putative CEBPD motifs at sites 1–6 of the PTX3 promoter (see panel (A), in vitro-translated HA-CEBPD protein, and specific CEBPD antibodies as indicated. “NS” indicates a nonspecific binding complex, “S” indicates the specific CEBPD-DNA complex, and “SS” indicates the supershift with the CEBPD antibody. (D) Both sites 1 and 5 of the PTX3 promoter are important for regulation by CEBPD. Schematic representation of the PTX3 reporters with single or double mutations (dashed boxes) in CEBPD-binding sites (left panel) cotransfected with CEBPD into U373MG cells. Lysates were prepared 12 hours after transfection and assayed for luciferase activity (right panel) (mean  $\pm$  SD,  $n = 3$ , \*\*  $p < 0.01$  by Student  $t$  test).



**Fig. 6.** CEBPD binds to the *PTX3* promoter in vivo. Chromatin immunoprecipitation (ChIP) assays were performed with THP-1 and U373MG cells treated for 3 hours with proinflammatory factors as indicated (20 ng/mL tumor necrosis factor alpha [TNF- $\alpha$ ] or 5 ng/mL interleukin [IL]-1 $\beta$ ). The schematic on the top indicates the location of the primers used for detection of the *PTX3* promoter by polymerase chain reaction (PCR). The graph on the right shows the results obtained from 3 independent experiments.



**Fig. 7.**

PTX3 inhibits phagocytosis of apoptotic cells by macrophages and enhances the apoptosis of SH-SY5Y cells. (A) Recombinant PTX3 protein was incubated with differentiated THP-1 cells, labeled in green by F4/80, and ultraviolet (UV)-damaged dead SH-SY5Y cells, labeled in red by PKH-26. The phagocytosis of dead SH-SY5Y cells by macrophages was monitored by flow cytometry. The percentage of phagocytosed SH-SY5Y cells under each condition was expressed as the mean  $\pm$  standard deviation from 3 independent experiments (mean  $\pm$  SD,  $n = 3$ , \*  $p < 0.05$ ; \*\*  $p < 0.01$  by Student  $t$  test). (B) Incubation with PTX3 enhanced the accumulation of dying SH-SY5Y cells. Recombinant PTX3 protein as indicated was incubated with differentiated THP-1 cells and serum starvation-treated, dying SH-SY5Y cells, labeled in red by PKH-26. The amount of SH-SY5Y cell apoptosis was assessed by PI staining, followed by flow cytometry. Results from a representative experiment are shown in the left panel. The increase of apoptosis with PTX3 relative to controls without PTX3 is shown on the right (mean  $\pm$  SD,  $n = 3$ ).

**Table 1**

CEBPD-responsive genes in U373MG cells

Function	Up-regulated genes	Down-regulated genes
Inflammation	<i>ID2, BCL2L1, CXCR4, CASP8, ITGA2, ALB, KITLG, ABCA1, EGR3, MMP1</i>	<i>FGF4, ABL1, ADAMTS13, THBS1, SYK, BCL2L1, AKT1, BAX, DTX1, SRF</i>
Neurological disease	<i>ID2, BCL2L1, SLC1A1, CXCR4, CHRNA3, CASP8, ITGA2, GABRE, KITLG, MMP1, MAOB, BARHL1, MT1E, MT1F</i>	<i>CACNA2D2, CHRND, NFATC4, BCL2L1, ALK, GDNF, AKT1, CDK2, BAX, PTPRF</i>
Cell death	<i>BMF, ID2, PDGFRA, SKI, BCL2L1, CXCR4, CEBPA, MMP10, CASP8, MYC, ALB, KITLG, CEBPE, CA2, PRLR, EGR3, MMP1, MT1E, MMP3, MT1F</i>	<i>SERPINC1, CACNA2D2, ALDH1A2, FGF4, KRT18, IRF5, ANKS1B, RPS6KA5, THBS1, CTGF, STK11, SYK, BCL2L1, GDNF, ABCB1, AKTI, BAX, SRF</i>
Hematological disease	<i>PDGFRA, BCL2L1, CXCR4, ALDOA, CEBPA, CHRNA3, CASP8, MYC, ALB, KITLG, PTX3, CEBPE, ABCA1, PRLR, EGR3, MT1E, MT1F</i>	<i>SERPINC1, FGF4, ADAMTS13, IRF5CHRND, THBS1, CTGF, IL1RAP, SYK, HSD11B1, BCL2L1, GDNF, ABCB1, AKTI, BAX</i>
Cellular growth and proliferation	<i>BMF, ID2, PDGFRA, SKI, BCL2L1, CXCR4, CEBPA, TNFAIP6, CASP8, MYC, ALB, KITLG, PTX3, CEBPE, RGS2, PRLR, EGR3, MT1E, MMP3, MT1F</i>	<i>SERPINC1, CACNA2D2, ALDH1A2, FGF4, CD163, THBS1, CTGF, STK11, SYK, HSD11B1, BCL2L1, GDNF, ABCB1, AKTI, BAX, SRF</i>
Others	<i>IL22RA1, CCL26, MARK1, LHX6, ETV1, ADAMTS5, S100A5, LRRK2, RHOU, ME1, APOL6, RGS16, IL1F7, NOX3, NPL, RIMS3, MT1M</i>	<i>SRI, RIMS1, APOF, ME3, SENP7, ABCBU, ETV7, ADAMDEC1, SEPT3, ADAM 11, AP0BEC3D, BZRAP1</i>